A Schwarz waveform relaxation method for time-dependent space fractional Schrödinger/heat equations

Xavier Antoine, Emmanuel Lorin

A Schwarz waveform relaxation method for time-dependent space fractional Schrödinger/heat equations

Xavier ANTOINE[a], Emmanuel LORIN[b,c]

[a] *Université de Lorraine, CNRS, Inria, IECL, F-54000 Nancy, France*
[b] *School of Mathematics and Statistics, Carleton University, Ottawa, Canada, K1S 5B6*
[c] *Centre de Recherches Mathématiques, Université de Montréal, Montréal, Canada, H3T 1J4*

Abstract

This paper is dedicated to the derivation and analysis of a Schwarz waveform relaxation domain decomposition method for solving time-dependent linear/nonlinear space fractional Schrödinger and heat equations. Along with the details of the derivation of the method and some mathematical properties, we also propose some illustrating numerical experiments and conjectures on the rate of convergence of the method.

Keywords: space fractional Schrödinger equation, space fractional heat equation, fractional Laplacian, domain decomposition method, Schwarz relaxation waveform algorithm.

Contents

Email addresses: xavier.antoine@univ-lorraine.fr (Xavier ANTOINE), elorin@math.carleton.ca (Emmanuel LORIN)

1. Introduction

In this paper, we derive and analyze a Schwarz Waveform Relaxation (SWR) Domain Decomposition Method (DDM) for the time-dependent linear space Fractional Schrödinger Equation (FSE): for all $(t,x) \in [0;T] \times \Omega$, with maximal time $T > 0$, and a one-dimensional bounded domain $\Omega \subseteq \mathbb{R}$, compute $u := u(t,x)$ solution to

$$\mathtt{i}\partial_t u + (-\triangle)^{\alpha/2} u + V(x)u = 0, \;\; u(0,x) = u_0(x), \;\; u(t,\partial\Omega) = 0\,, \tag{1}$$

with fractional exponent $\alpha \in (0,2)$ and setting $\mathtt{i} := \sqrt{-1}$. The spatial potential is described by a function $V \in L^\infty(\Omega)$. We set homogeneous Dirichlet boundary conditions but the extension to other kinds of boundary conditions can be also considered. The initial data is a given function u_0 in Ω. Let us recall that the Riemann-Liouville-based definition of the fractional Laplace operator in d-dimension reads (see [55]), for $\alpha \in (0,2)$ and any $u \in \mathcal{S}(\mathbb{R}^d)$, as follows

$$(-\triangle)^{\alpha/2} u(\boldsymbol{x}) = C(\alpha) \lim_{\varepsilon \to 0^+} \int_{\mathbb{R}^d \setminus B_\varepsilon(\boldsymbol{x})} \frac{u(\boldsymbol{x}) - u(\boldsymbol{y})}{|\boldsymbol{x} - \boldsymbol{y}|^{d+\alpha}} d\boldsymbol{y}, \tag{2}$$

where $B_\varepsilon(\boldsymbol{x})$ is the ball of radius ε and center $\boldsymbol{x}$, $C(\alpha)$ is the constant defined by

$$C(\alpha) \;\; := \;\; \Big(\int_{\mathbb{R}^d} \frac{1 - \cos(\xi_1)}{|\boldsymbol{\xi}|^{d+\alpha}} d\boldsymbol{\xi} \Big)^{-1}, \tag{3}$$

with $\boldsymbol{\xi} := (\xi_1, ..., \xi_d) \in \mathbb{R}^d$. In addition, for system (1) but set in $\Omega := \mathbb{R}^d$, i) the mass

$$\mathcal{N}(t) := \int_\Omega |u|^2 d\Omega = \int_\Omega |u_0|^2 d\Omega, \forall t > 0, \tag{4}$$

and ii) the total energy

$$\mathcal{E}(t) := \frac{1}{2} \int_\Omega \bar{u} (-\triangle)^{\alpha/2} u d\Omega + \int_\Omega V(x) |u|^2 d\Omega = \mathcal{E}(t=0), \forall t > 0, \tag{5}$$

which is the sum of the fractional kinetic energy and the potential energy, are both conserved. For $\Omega := \mathbb{R}^d$, some definitions of the fractional Laplacian can be equivalent [41] and, for example for the Fourier spectral definition of the fractional Laplace operator, conservations properties as well as dynamical laws can be proved for nonlinear fractional Schrödinger and Gross-Pitaevskii equations (see e.g. [11, 12] and Subsection 4.2). For a bounded domain, this is less clear and strongly depends on the definition of the fractional laplacian as well as the boundary conditions, which can lead to definitions which are no longer equivalent. Finally, the well-posedness of different versions of the fractional linear and nonlinear Schrödinger equations can be found for instance in [21, 29, 31, 60, 62].

The space FSE was initially introduced by Laskin [42, 43, 44]. Some important impacts concern fractional quantum dynamics based on the space or/and time Fractional Schrödinger equation and some nonlinear versions [1, 14, 18, 20, 22, 24, 36, 48, 53, 57, 65]. The fractional

nonlinear Schrödinger equation is used to describe the nonlocal phenomena in quantum physics and to explore the quantum behaviors of either long-range interactions or time-dependent processes involving many scales [1, 13, 39, 40, 42, 43, 44, 48, 53, 61, 67]. For example, the nonlinear FSE is met when modeling quantum fluids of light [20], boson stars [14, 24, 36] and polariton condensates [57]. Additional applications can also be found in linear and nonlinear optics [68, 69] to understand the propagation of super-Gaussian beams. Therefore, designing efficient and accurate schemes to numerically compute the solution to such equations is of great interest.

During the past two decades, there has been a huge interest in computational methods for solving fractional PDEs including fractional Laplace, heat and Schrödinger equations [11, 12, 19, 23, 32, 38, 39, 46, 47, 52, 58, 59, 63, 64]. Practically, the choice of the computational method largely depends on the definition of the fractional Laplace operator. When using the spectral definition of the fractional derivatives, the numerical computation can for instance (at least with null Dirichlet boundary conditions) be reduced to solving fractional linear algebraic systems $A^\alpha x = b$ [9, 10, 49]. Alternatively, the fractional Laplacian definition using Fourier-based fractional derivatives (Riesz) can be approximated using standard FFT [10]. Riemann-Liouville or Caputo's based fractional derivatives are usually more difficult to numerically deal with. The latter are indeed defined by nonlocal integro-differential operators which require very special care in order to derive stable, accurate and efficient finite-difference or finite element solvers. We refer again to [47] for an overview of definitions and computational methods for the fractional Laplacian. Here, we use the method presented in [35] for approximating the fractional Laplace operator (2).

In the present paper, we propose to derive and analyze a non-overlapping Schwarz Waveform Relaxation DDM for solving (1) in parallel (see e.g. [3, 25, 26, 27, 28, 30, 50]). Most of the analysis and methods proposed here can actually be easily adapted to the fractional heat equation (as seen in Section 6). Let us remark that, to the best of the authors' knowledge, the only work related to DDM for fractional PDEs is [37]. In this contribution, the authors use additive Schwarz DDM on the algebraic discrete system for stationary fractional PDEs.

To start, we recall some basic facts about the SWR algorithm for solving a one-dimensional evolution PDE: $Pu = 0$, with $u(0,\cdot) = u_0$, on two subdomains $\Omega^\varepsilon_\pm$, with boundary at $\pm\varepsilon/2$ ($\varepsilon \geqslant 0$) such that $\Omega = \Omega^\varepsilon_+ \cup \Omega^\varepsilon_-$ and overlapping region $\Omega^\varepsilon_+ \cap \Omega^\varepsilon_- = (-\varepsilon/2, \varepsilon/2)$. Solving the SWR DDM requires some transmission conditions at the subdomain interfaces. More specifically, for any Schwarz iteration $k \geqslant 1$, the equation in $\Omega^\varepsilon_\pm$ reads

$$\left\{\begin{array}{lcl} Pu^{(k)}_\pm & = & 0, \ \text{ on } [0,T]\times\Omega^\varepsilon_\pm, \\ \mathcal{B}_\pm u^{(k)}_\pm & = & \mathcal{B}_\pm u^{(k-1)}_\mp, \ \text{ at } [0,T]\times\{\pm\varepsilon/2\}, \\ u^{(k)}_\pm(0,\cdot) & = & u_0(\cdot) \ \text{ on } \Omega^\varepsilon_\pm. \end{array}\right. \tag{6}$$

The notation $u^{(k)}_\pm$ stands for the solution $u_\pm$ in $[0,T]\times\Omega^\varepsilon_\pm$ at Schwarz iteration $k \geqslant 0$. The key-point from the parallel computing point of view is the decoupling at Schwarz iteration k, of the two systems thanks to the transmission conditions involving data from the $(k-1)$-th

Schwarz iteration on the right hand side of the second equation of (6). Initially, $u_{\pm}^{(0)}$ are two given functions defined in $\Omega_{\pm}^{\varepsilon}$, typically taken null if no further information is provided. The operator $\mathcal{B}_{\pm}$ characterizes the type of SWR algorithm. In the Classical SWR (CSWR) case, $\mathcal{B}_{\pm}$ is simply the identity operator, $\mathcal{B}_{\pm} = \pm\partial_x + \gamma \mathrm{Id}$ ($\gamma \in \mathbb{R}_+^*$) for the Robin SWR, and $\mathcal{B}_{\pm}$ is a nonlocal Dirichlet-to-Neumann-like (DtN) pseudodifferential operator for the Optimal SWR (OSWR). We refer to [4, 5, 6, 7, 8, 16, 30] for further reading for the case of the Schrödinger equation.

The rest of the paper is organized as follows. In Section 2, we present the numerical scheme for the discretization of the FSE, preserving both the mass and energy. In addition, the error on the scheme is given and numerical simulations allow to check the main properties. In Section 3, we derive the Schwarz waveform relaxation DDM. Its computational complexity is analyzed and its convergence is stated. Some numerical experiments, for the linear and nonlinear FSE, and a conjecture on the rate of convergence are proposed in Section 4. In Section, 5, we provide a straightforward extension of the proposed SWR DDM to the fractional heat equation. We conclude in Section 6.

2. Numerical discretization of the space FSE

The proposed numerical scheme is based on the finite-difference discretization of the fractional Laplace operator (2) which was derived and analyzed in [35]. We denote by $\{u_j^n\}_j$ a sequence of approximations of $\{u(t_n, x_j)\}_j$, for an equally spaced finite-difference grid $\{x_j\}_j$ with mesh size Δx, and for the discrete times $t_0 < t_1 < \cdots < t_n := n\Delta t < \cdots \leqslant T$, with fixed time step Δt such that $N\Delta t = T$. The proposed Crank-Nicolson(CN) based scheme for (1) hence reads

$$\begin{aligned} u_i^{n+1} &= u_i^n + \frac{\mathtt{i}\Delta t}{2}\sum_{j\geqslant 1}(2u_i^n - u_{i+j}^n - u_{i-j}^n)w_j^{F,G} + \frac{\mathtt{i}\Delta t}{2}\sum_{j\geqslant 1}(2u_i^{n+1} - u_{i+j}^{n+1} - u_{i-j}^{n+1})w_j^{F,G} \\ &\quad + \frac{\mathtt{i}\Delta t}{2}V_j(u_i^n + u_i^{n+1})\,, \end{aligned} \tag{7}$$

where according to [35], for any $j \in \mathbb{Z}$ the weights w_j^F are given by

$$w_j^F = \Delta x^{-\alpha}\begin{cases} \dfrac{C_{1,\alpha}}{2-\alpha} - F'(1) + F(2) - F(1), \ j = \pm 1\,, \\ F(j+1) - 2F(j) + F(j-1), \ j = \pm 2, \pm 3, \cdots \end{cases} \tag{8}$$

with

$$F(t) = \begin{cases} \dfrac{C_{1,\alpha}}{\alpha(\alpha-1)}|t|^{1-\alpha}, \ \alpha \neq 1 \\ -C_{1-\alpha}\log|t|, \ \alpha = 1 \end{cases}, \ C_{1,\alpha} = \frac{2^{\alpha-1}\alpha\Gamma\Big(\dfrac{\alpha+1}{\alpha}\Big)}{\pi^{1/2}\Gamma\Big(\dfrac{2-\alpha}{2}\Big)},$$

designating by Γ the Gamma special function. Alternatively, it is possible to get a higher order approximation of the fractional Laplacian thanks to the following weights: for any

$j \in \mathbb{Z}$

$$w_j^G = \Delta x^{-\alpha} \begin{cases} \dfrac{C_{1,\alpha}}{2-\alpha} - G''(1) - \dfrac{G'(3)+3G'(1)}{2} + G(3) - G(1) \;\; j = \pm 1\,, \\ 2\big(G'(j+1) + G'(j-1) - G(j+1) + G(j-1)\big), \;\; j = \pm 2, \pm 4, \cdots \\ -\dfrac{G'(j+2)+6G'(j)+G'(j-2)}{6} + G(j+2) - G(j-2), \;\; j = \pm 3, \pm 5, \cdots \end{cases} \tag{9}$$

with

$$G(t) \;\; = \;\; \begin{cases} \dfrac{C_{1,\alpha}}{\alpha(\alpha-1)(2-\alpha)} |t|^{2-\alpha}, \;\; \alpha \neq 1\,, \\ C_{1-\alpha}(t - \log|t|), \;\; \alpha = 1\,. \end{cases}$$

For instance, we report in semilogscale on Fig. 1 the values of the weights $\{w_j^F\}_{1 \leqslant j \leqslant J}$ and $\{w_j^G\}_{1 \leqslant j \leqslant J}$, for $J = 50$.

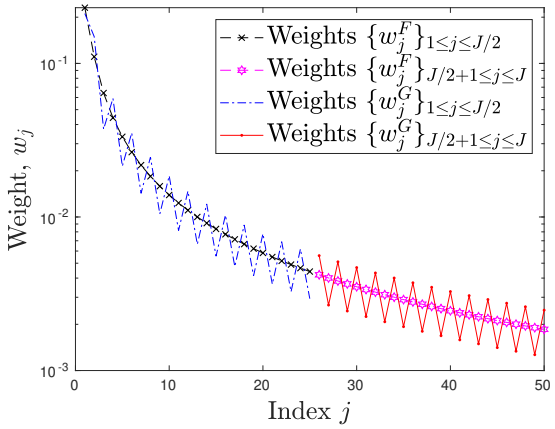

Figure 1: Weights $\{w_j^F\}_{1 \leqslant j \leqslant J}$ and $\{w_j^G\}_{1 \leqslant j \leqslant J}$ (for $J = 50$) used in the fractional Schrödinger equation solver.

For $n \neq 1$, $\boldsymbol{u}^0$ given as the projection of u_0 on the finite-difference grid $\{x_j = j\Delta x\}_{j \in \mathcal{J}}$, setting $\mathcal{J} = \{-J/2+1 \leqslant j \leqslant J/2\}$, and with homogeneous Dirichlet boundary conditions at the ghost points $x_{-J/2}$ and $x_{J/2+1}$ ($J \in 2\mathbb{N}$ and $\Omega = [x_{-J/2}; x_{J/2+1}]$), the scheme can simply be rewritten in the form

$$\Big(\boldsymbol{I} + \frac{\mathtt{i}\Delta t}{2}\boldsymbol{A}_V\Big)\boldsymbol{u}^{n+1} \;\; = \;\; \Big(\boldsymbol{I} - \frac{\mathtt{i}\Delta t}{2}\boldsymbol{A}_V\Big)\boldsymbol{u}^n\,, \tag{10}$$

where $\boldsymbol{A}_V = \boldsymbol{A} + \boldsymbol{V} \in \mathbb{R}^{J \times J}$ is the full real-valued symmetric matrix, $\boldsymbol{A}$ is the full positive definite (SPD) $J \times J$ matrix with coefficients deduced from (7) for the fractional Laplacian, and $\boldsymbol{V}$ is the diagonal matrix part representing the potential. More specifically, the entries

of $\boldsymbol{A}$ are defined as follows: $A_{i,i} = 2\sum_{1\leqslant j\leqslant J} w_j^{F,G}$ and $A_{i,i-j} = -w_j^{F,G}$ for $1 \leqslant j \leqslant i-1$ and $A_{i,i+j} = -w_j^{F,G}$ for $1 \leqslant j \leqslant J-i$. The complex-valued vector is $\boldsymbol{u}^n = (u_j^n)_{j\in\mathcal{J}}^T \in \mathbb{C}^J$. This scheme trivially conserves the mass, for all $n \in \mathbb{N}$,

$$\mathcal{N}^{n+1} := \|\boldsymbol{u}^{n+1}\|_{2,J}^2 = \|\boldsymbol{u}^n\|_{2,J}^2 =: \mathcal{N}^n, \tag{11}$$

where the $\ell^{2,J}$-norm is defined by

$$\|\boldsymbol{u}\|_{2,J} = (\boldsymbol{u},\boldsymbol{u})_{2,J}^{1/2} := \sqrt{\Delta x}(\sum_{j\in\mathcal{J}} |u_j|^2)^{1/2},$$

and the inner product by

$$(\boldsymbol{u},\boldsymbol{v})_{2,J} := \Delta x \sum_{j\in\mathcal{J}} u_j\overline{v_j}\,, \tag{12}$$

with $\boldsymbol{u} \in \mathbb{C}^J$ and $\boldsymbol{v} \in \mathbb{C}^J$. Let us define now the discrete fractional energy by

$$\mathcal{E}^n := \frac{1}{2}(\boldsymbol{A}\boldsymbol{u}^n,\boldsymbol{u}^n)_{2,J} + (\boldsymbol{V}\boldsymbol{u}^n,\boldsymbol{u}^n)_{2,J}. \tag{13}$$

Then, since $\boldsymbol{A}$ is SPD, we can easily deduce that the discrete fractional energy conservation holds

$$\mathcal{E}^n = \mathcal{E}^0, \forall n \in \mathbb{N}, \tag{14}$$

by adapting the proof from [59, 63, 64]. It is also possible to use a standard first-order backward Euler scheme in time following

$$\big(\boldsymbol{I} + \mathtt{i}\Delta t\boldsymbol{A}_V\big)\boldsymbol{u}^{n+1} \;\; = \;\; \boldsymbol{u}^n\,. \tag{15}$$

Let us now define the uniform norm

$$||\boldsymbol{u}||_{\infty,J} = \max_{j\in\mathcal{J}} |u_j|\,, \tag{16}$$

and the infinite norm error

$$e(\Delta t,\Delta x) := \max_{0\leqslant n\leqslant N} ||\boldsymbol{u}^n - \boldsymbol{u}_{\rm ref}^n||_{\infty,J},$$

where $\boldsymbol{u}_{\rm ref}^n$ is the exact solution at time t_n evaluated at the J spatial grid points. Based on [35] and standard results, we get the following proposition.

Proposition 2.1. *The CN scheme* (10) *(resp. backward Euler scheme* (15)*) constructed from* (7) *is consistent with* (1)*, unconditionally stable, and its truncation error* $e(\Delta t,\Delta x)$ *is such that*

- *if the weights* $\{w_j\}_j$ *are given by* (8)*, then:* $e(\Delta t,\Delta x) = O(\Delta x^{2-\alpha}) + O(\Delta t^2)$ *(resp.* $e(\Delta t,\Delta x) = O(\Delta x^{2-\alpha}) + O(\Delta t)$*).*

- *if* $\{w_j\}_j$ *are defined from* (9)*, then:* $e(\Delta t, \Delta x) = O(\Delta x^{3-\alpha}) + O(\Delta t^2)$ *(resp.* $e(\Delta t, \Delta x) = O(\Delta x^{3-\alpha}) + O(\Delta t)$*).*

In order to illustrate the order of convergence of the scheme and to check the conservation laws, we consider the discretization to (1) for $\alpha = 0.5$ on the computational domain $\Omega = (-10, 10)$. The initial condition is $u_0(x) = \exp(-10x^2 + 2\mathtt{i}x)$ and we take $V = 0$. We use the F-scheme (8) for the Crank-Nicolson approximation in time. Theoretically, the expected order of convergence in space for the scheme (7) with the F-weights is $2 - \alpha = 1.5$ (see [35]) and 2 in time. Numerically, we test the spatial convergence by making vary the number of grid points J from 32 to 4096. The final time is set to $T = 5 \times 10^{-1}$ and the time step is $\Delta t = 10^{-2}$. We report in logscale in Fig. 2 (Left) the absolute $\ell^{2,J}$-norm error $\|\boldsymbol{u}^N_{\text{ref}} - \boldsymbol{u}^N\|_{2,J}$ at final time $t_N = T$ as a function of the space step Δx, where the reference solution $\boldsymbol{u}^N_{\text{ref}}$ is computed on the finest mesh $\Delta x = 2^{-11}$. As expected, we numerically obtain a convergence order in space close to 1.5. Regarding the convergence in time, we fix the number of grid points to $J = 1024$ and final time to $T = 2.5 \times 10^{-1}$. The time step Δt varies from 2^{-7} to 2^{-11}. We report the absolute $\ell^{2,J}$-norm error at final time in logscale as a function of Δt in Fig. 2 (Right). The convergence in time is close to 2, as theoretically expected.

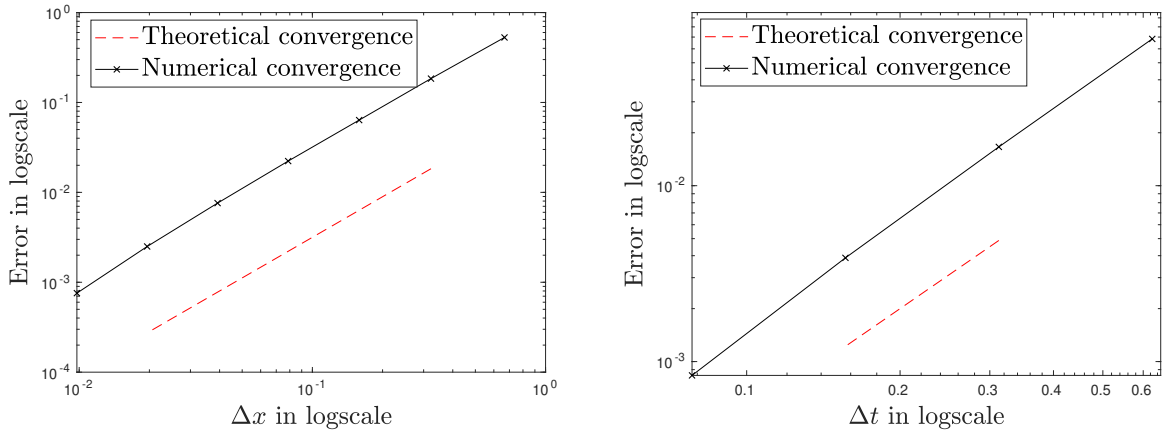

Figure 2: (Left) Theoretical and numerical $\ell^{2,J}$-norm error vs Δx. (Right) Theoretical and numerical $\ell^{2,J}$-norm error vs Δt.

Finally, in Fig. 3 we report the relative variation of the mass (resp. energy) $|\mathcal{N}^n - \mathcal{N}^0|/\mathcal{N}^0$ (resp. $|\mathcal{E}^n - \mathcal{E}^0|/\mathcal{E}^0$) as a function of the time iteration, n. In this test, we have taken the same data as above, with $\Delta t = 10^{-2}$ and $J = 500$. This example numerically illustrates the very good conservation of both the discrete mass and fractional energy as functions of time.

3. Domain decomposition method for the space FSE

In this section, we derive the SWR method and analyze its convergence and computational complexity. Some illustrative numerical examples are then proposed and convergence

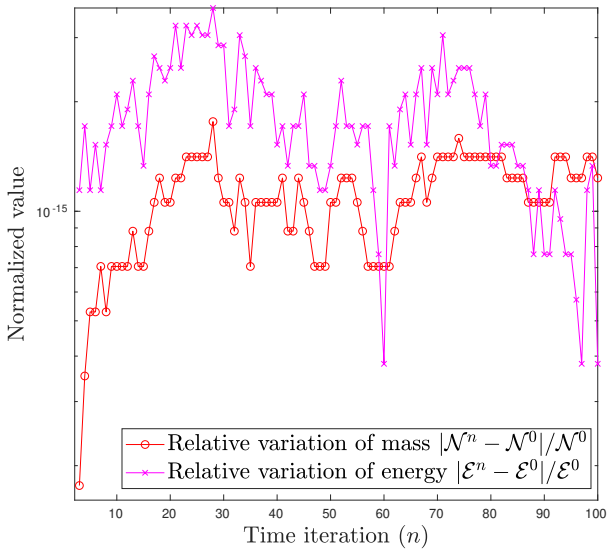

Figure 3: Evolution of the relative variation of the discrete mass and energy vs n.

properties are numerically exhibited.

3.1. Derivation of the SWR DDM for the FSE

We describe here a non-overlapping Schwarz waveform relaxation ($\varepsilon = 0$) method for solving (1) on $\Omega = \Omega_- \cup \Omega_+$ (with $\Omega_- \cap \Omega_+ = \emptyset$). We recall that $u_\pm^{(k)}$ denotes the solution in $\Omega_\pm$ at Schwarz iteration $k \geqslant 0$. For technical reasons, $u_\pm$ is defined in all $[0,T]\times\Omega$, although it is only updated from computations in $\Omega_\pm$. Moreover, $u_\pm^{(0)}$ is initially set to zero. We then solve for $k \geqslant 1$

$$\begin{aligned} \mathtt{i}\partial_t u_\pm^{(k)} + (-\triangle)^{\alpha/2} u_\pm^{(k)} + V(x) u_\pm^{(k)} &= 0,\ (t,x) \in [0,T]\times\Omega_\pm\,, \\ u_\pm^{(k)} &= u_\mp^{(k-1)},\ (t,x) \in [0,T]\times\Omega_\mp\,. \end{aligned}$$

Denoting by $u_{\pm;i}^{n;(k)}$ the approximate solution at Schwarz iteration k, time t_n and point x_i, the numerical scheme, for $1 \leqslant i \leqslant J/2$, reads as follows in Ω_+

$$\begin{aligned} u_{+;i}^{n+1;(k)} = u_{+;i}^{n;(k)} - \frac{\mathtt{i}\Delta t}{2}\Big[&\textstyle\sum_{j\geqslant 1}\big(u_{+;i}^{n;(k)} - u_{+;i+j}^{n;(k)}\big)w_j + \sum_{j\geqslant 1}\big(u_{+;i}^{n+1;(k)} - u_{+;i+j}^{n+1;(k)}\big)w_j \\ &\textstyle\sum_{1\leqslant j\leqslant i-1}\big(u_{+;i}^{n;(k)} - u_{+;i-j}^{n;(k)}\big)w_j + \sum_{j\geqslant i}\big(u_{+;i}^{n;(k)} - u_{-;j}^{n;(k-1)}\big)w_j\Big] \\ &+ \frac{\mathtt{i}\Delta t}{2} V_i^+ (u_{+;i}^{n;(k)} + u_{+;i}^{n+1;(k)}), \end{aligned} \tag{17}$$

where $V_i^+ = V(x_i)$, and in Ω_- as

$$\begin{aligned} u_{-;i}^{n+1;(k)} &= u_{-;i}^{n;(k)} - \frac{\mathtt{i}\Delta t}{2}\Big[\sum_{j\geqslant 1}\big(u_{-;i}^{n;(k)} - u_{-;i-j}^{n;(k)}\big)w_j + \sum_{j\geqslant 1}\big(u_{-;i}^{n+1;(k)} - u_{-;i-j}^{n+1;(k)}\big)w_j \\ &\quad + \sum_{1\leqslant j\leqslant J/2-i}\big(u_{-;i}^{n;(k)} - u_{-;i+j}^{n;(k-1)}\big)w_j + \sum_{j>J/2-i}\big(u_{-;i}^{n;(k)} - u_{+;j}^{n;(k-1)}\big)w_j\Big] \\ &\quad + \frac{\mathtt{i}\Delta t}{2}V_i^-(u_{-;i}^{n;(k)} + u_{-;i}^{n+1;(k)})\,, \end{aligned} \tag{18}$$

where $V_i^- = V(x_{i-J/2})$ and w_j designates one of the weights (8) or (9). These schemes can simply be rewritten, for all $k \geqslant 1$ until convergence, as

$$\Big(\boldsymbol{I} + \frac{\mathtt{i}\Delta t}{2}\boldsymbol{A}_{V,\pm}\Big)\boldsymbol{u}_{\pm}^{n+1;(k)} = \Big(\boldsymbol{I} - \frac{\mathtt{i}\Delta t}{2}\boldsymbol{A}_{V,\mp}^T\Big)\boldsymbol{u}_{\pm}^{n;(k)} + \boldsymbol{F}_{\pm}^{n+1;(k-1)} + \boldsymbol{F}_{\pm}^{n;(k-1)}\,, \tag{19}$$

where $\boldsymbol{A}_{V,+} = \boldsymbol{A}_{V,-}^T \in \mathbb{R}^{J/2\times J/2}$ and $\boldsymbol{F}_{\pm}^{n;(k-1)} \in \mathbb{C}^{J/2}$ are constructed from (17) and (18). Alternatively, a backward Euler scheme in time reads

$$\big(\boldsymbol{I} + \mathtt{i}\Delta t\boldsymbol{A}_{V,\pm}\big)\boldsymbol{u}_{\pm}^{n+1;(k)} = \boldsymbol{u}_{\pm}^{n;(k)} + \boldsymbol{F}_{\pm}^{n+1;(k-1)}\,. \tag{20}$$

Regarding the convergence criterion, we denote by $\boldsymbol{v}^{n;(k)} = \{v_j^{n;(k)}\}_j$ the concatenation of $\boldsymbol{u}_-^{n;(k)}$ and $\boldsymbol{u}_+^{n;(k)}$. We stop the iteration in k when the following relative error is less than a small enough prescribed parameter $\delta > 0$,

$$\max_{1\leqslant n\leqslant N_T}\frac{\|\boldsymbol{v}^{n;(k)} - \boldsymbol{v}^{n;(k-1)}\|_{2;J}}{\|\boldsymbol{v}^{n;(k)}\|_{2;J}} \leqslant \delta\,, \tag{21}$$

where we have defined

$$v_j^{n;(k)} = \begin{cases} u_{-;j+J/2}^{n;(k)}, & \text{if } -J/2+1 \leqslant j \leqslant 0, \\ u_{+;j}^{n;(k)}, & \text{if } 1 \leqslant j \leqslant J/2. \end{cases}$$

There are three main advantages of the proposed method:

- No overlap is needed ($\Omega_+ \cap \Omega_- = \emptyset$).
- The algorithm is embarrassingly parallel, thanks to the Schwarz waveform relaxation approach.
- The transmission condition is trivial to implement and is computationally very cheap.

3.2. Computational complexity

In order to compute the local solution $u_{\pm}^{(k)}$ at Schwarz iteration k in a given domain $\Omega_\pm$, it is necessary to have access to the solution $u_{\mp}^{(k-1)}$ at the previous iteration $(k-1)$ in the complementary subdomain $\Omega_\mp$; this is indeed necessary to compute both $\boldsymbol{F}_{\pm}^{n;(k-1)}$ and $\boldsymbol{F}_{\pm}^{n+1;(k-1)}$. The term $\boldsymbol{F}_{\pm}^{(k-1)}$ is computed by the processors of the node where $u_{\mp}^{(k-1)}$ is stored

and updated. Then, at time iteration $n+1$, we only transfer $\boldsymbol{F}_{\pm}^{n;(k-1)}$ and $\boldsymbol{F}_{\pm}^{n+1;(k-1)}$ from $\Omega_{\mp}$ to $\Omega_{\pm}$ in order to update $\boldsymbol{u}_{\pm}^{n+1;(k-1)}$ (see also (19)).

In order to specify the overall computational complexity, let us discuss this question for $\mathtt{P}$ non-overlapping subdomains $\cup_{\mathtt{p}=1}^{\mathtt{P}}\Omega_{\mathtt{p}} = \Omega$, with corresponding solutions $u_{\mathtt{p}}^{n;(k)}$ on a $\mathtt{P}$ node/processor computer. By default on a spatial grid with J points and for N_T time iterations, the overall complexity of the direct implicit Crank-Nicolson fractional Schrödinger equation solver is $O(N_T J^3)$, since $(\boldsymbol{I}+\mathtt{i}\Delta t/2\mathbf{A}_V) \in \mathbb{R}^{J\times J}$ is a full matrix. The SWR method requires to solve in parallel $\mathtt{P}$ local FSEs on grids involving $J/\mathtt{P}$ points. However, in addition to solving these local FSEs, it is also necessary to compute the transmitted information *via* the right hand sides (corresponding for instance to $\boldsymbol{F}_{\pm}^{n+1;(k-1)}$ in (19) when $\mathtt{P}=2$). For each processor $\mathtt{l} \in \{1,\cdots,\mathtt{P}\}$, at each Schwarz iteration k and any time step $n+1$, we need

- to solve a full $J/\mathtt{P} \times J/\mathtt{P}$ linear system, which requires $O\big((J/\mathtt{P})^3\big)$ operations,
- to compute $\boldsymbol{F}_{\mathtt{lp}}^{n;(k-1)}$ for each $\mathtt{p} \in \{1,\cdots,\mathtt{P}\}\backslash\{\mathtt{l}\}$, corresponding to the contribution from the $(k-1)$-th Schwarz iteration which must be sent to the $(\mathtt{P}-1)$ other processors for computing the solution in $\Omega_{\mathtt{p}}$. Each term $\boldsymbol{F}_{\mathtt{lp}}^{n;(k)}$ requires $O(J/\mathtt{P})$ operations, for a total of $O(J)$ operations for Processor $\mathtt{l}$.

This leads to the following proposition.

Proposition 3.1. *Consider the backward Euler* (20) *or the Crank-Nicolson scheme* (19) *for solving the FSE* (1)*. Then, for N_T time iterations and for a spatial grid with J points, the computational complexity of the sequential solver* (10) *is $O(N_T J^3)$. On $\mathtt{P}$ processors, and assuming that the SWR method requires k_δ iterations to converge up to a prescribed tolerance δ, the overall computational complexity is $O\big(N_T k_\delta (J^3/\mathtt{P}^2 + \mathtt{P}J)\big)$. The SWR DDM is hence efficient as long as $k_\delta = o(\mathtt{P}^2)$ and $k_\delta = o\big(J^2/\mathtt{P}\big)$.*

Regarding the data transmission, for each processor $\mathtt{l} \in \{1,\cdots,\mathtt{P}\}$, each Schwarz iteration and each time iteration, it is necessary to transmit $\mathtt{P}-1$ vectors of size $J/\mathtt{P}$ to the other $\mathtt{P}-1$ processors, while it is needed to store the *local solutions* at anytime, which can potentially be problematic from the memory point of view.

3.3. Convergence analysis of the SWR DDM for the FSE

We now establish the convergence of the SWR DDM derived above.

Proposition 3.2. *For any $\boldsymbol{u}_{\pm}^{n;(0)}$, the algorithms* (19) *and* (20) *with null potential ($V=0$) are convergent.*

Proof. Let us study the convergence of (20). The Crank-Nicolson version is a little bit more technical but is fundamentally similar. In order to study the convergence of the algorithm, let us rewrite the scheme (20) as follows

$$\big(\boldsymbol{I} + \mathtt{i}\Delta t \boldsymbol{A}_{\pm}\big)\boldsymbol{u}_{\pm}^{n+1;(k)} \;=\; \boldsymbol{u}_{\pm}^{n;(k)} - \mathtt{i}\Delta t \boldsymbol{B}_{\pm}\boldsymbol{u}_{\mp}^{n+1;(k-1)}, \tag{22}$$

where the matrices $\boldsymbol{B}_+$ and $\boldsymbol{B}_- = \boldsymbol{B}_+^T \in \mathbb{R}^{J/2\times J/2}$ correspond to the contribution of the coefficients $\{w_j\}_{|j|>J/2}$. Let us define $\boldsymbol{v}^{n;(k)} = (\boldsymbol{u}_-^{n;(k)}, \boldsymbol{u}_+^{n;(k)})^T$ and

$$\boldsymbol{B} \;=\; \begin{pmatrix} \boldsymbol{I} + \mathtt{i}\Delta t \boldsymbol{A}_+^T & \boldsymbol{O} \\ \boldsymbol{O} & \boldsymbol{I} + \mathtt{i}\Delta t \boldsymbol{A}_+ \end{pmatrix}, \quad \boldsymbol{C} \;=\; -\mathtt{i}\Delta t \begin{pmatrix} \boldsymbol{O} & \boldsymbol{B}_+^T \\ \boldsymbol{B}_+ & \boldsymbol{O} \end{pmatrix}.$$

Thus, we have

$$\boldsymbol{B}\boldsymbol{v}^{n+1;(k)} \;=\; \boldsymbol{v}^{n;(k)} + \boldsymbol{C}\boldsymbol{v}^{n+1;(k-1)}.$$

Then, for $k \geqslant 2$, we obtain

$$\boldsymbol{v}^{n+1;(k)} - \boldsymbol{v}^{n+1;(k-2)} \;=\; \boldsymbol{B}^{-1}\big(\boldsymbol{v}^{n;(k)} - \boldsymbol{v}^{n;(k-2)}\big) + \boldsymbol{B}^{-1}\boldsymbol{C}\big(\boldsymbol{v}^{n+1;(k-1)} - \boldsymbol{v}^{n;(k-3)}\big).$$

We deduce that for any $k \geqslant 2$

$$\begin{aligned} \|\boldsymbol{v}^{n+1;(k)} - \boldsymbol{v}^{n+1;(k-2)}\|_{2,J} \;\leqslant\; & |||\boldsymbol{B}^{-1}||| \times \|\boldsymbol{v}^{n;(k)} - \boldsymbol{v}^{n;(k-2)}\|_{2,J} \\ & + |||\boldsymbol{B}^{-1}\boldsymbol{C}||| \times \|\boldsymbol{v}^{n+1;(k-1)} - \boldsymbol{v}^{n+1;(k-3)}\|_{2,J}. \end{aligned}$$

An induction argument on $n < N_T$ allows to conclude: indeed for $n = 1$, we simply use that $\boldsymbol{v}_\pm^{0;(k)} = \boldsymbol{u}_\pm^{(k)}(0,\cdot) = \boldsymbol{u}_{0|\Omega_\pm}$. Assuming that the convergence occurs at time iteration $n \geqslant 1$, there exists $0 < c_n < 1$, such that

$$\|\boldsymbol{v}^{n+1;(k)} - \boldsymbol{v}^{n+1;(k-2)}\|_{2,J} \;=\; |||\boldsymbol{B}^{-1}|||c_n^k + |||\boldsymbol{B}^{-1}\boldsymbol{C}||| \times \|\boldsymbol{v}^{n+1;(k-1)} - \boldsymbol{v}^{n;(k-3)}\|_{2,J}.$$

It is easy to deduce that there exists a positive constant $D > 0$, such that

$$\|\boldsymbol{v}^{n+1;(k)} - \boldsymbol{v}^{n+1;(k-2)}\|_{2,J} \;=\; Dc_n^k + |||\boldsymbol{B}^{-1}\boldsymbol{C}|||^{k-1} \times \|\boldsymbol{v}^{n+1,(1)} - \boldsymbol{v}^{n,(0)}\|_{2,J}.$$

By construction (see for instance Fig. 1), we trivially have $|||\boldsymbol{B}^{-1}\boldsymbol{C}||| < 1$, which allows us to conclude. □

The assumption on the potential easily ensures the convergence of the algorithm thanks to the fact that $|||\boldsymbol{B}^{-1}\boldsymbol{C}||| < 1$. In presence of a potential, we still expect this inequality to be satisfied, as long as Δt (or $\|V\|_\infty$) is small enough. Otherwise, the proof of convergence may require additional technical steps. At the purely continuous level, the convergence rate of the SWR method could possibly be improved by the construction of "local-in-space" transmission conditions, as it is the case for standard SWR methods applied to classical and quantum wave equations. The principle of the derivation of efficient (for fast convergence of the SWR solver) transmission conditions is often based on a Nirenberg factorization of the considered operator [33, 34, 56]. Such factorizations then allow to construct transparent-like transmission conditions. For the classical Schrödinger equation, these transmission conditions are typically Dirichlet-to-Neumann operators. We refer to [4, 5, 8, 30] for more details. Transparent-like transmission conditions for fractional Schrödinger equations will be investigated in future works. The starting point would then be, for constant potentials, the factorization of the fractional operator $P := \partial_t - \mathtt{i}V - \mathtt{i}(-\partial_x^2)^{\alpha/2}$ as follows

$$P \;=\; \big(\sqrt{\partial_t - \mathtt{i}V} - e^{\mathtt{i}\pi/4}(-\partial_x^2)^{\alpha/4}\big)\big(\sqrt{\partial_t - \mathtt{i}V} + e^{\mathtt{i}\pi/4}(-\partial_x^2)^{\alpha/4}\big),$$

which would lead to the corresponding transparent operators used as the transmission conditions based on $\sqrt{\partial_t - \mathtt{i}V} \pm e^{\mathtt{i}\pi/4}(-\partial_x^2)^{\alpha/4}$. Space-dependent potentials would require more advanced symbolic computation and pseudodifferential calculus (see for instance [5, 6, 56]).

4. Numerical examples

In this subsection, we propose some numerical examples illustrating the convergence of the SWR DDM, and we exhibit some properties related to the rate of convergence depending on α, Δt, and Δx. We start by analyzing in details the case of the linear FSE and then extend the algorithm to the nonlinear case to show its behavior.

4.1. The linear fractional Schrödinger equation

We propose a first convergence test for the non-overlapping SWR method previously developed with $\alpha = 0.5$ for the case of the linear FSE. The computational domain is $\Omega = (-4, 4)$, the initial data is $u_0(x) = \exp\big(-20x^2 + 5\mathtt{i}x\big)$ and the potential V is given by a gaussian well: $V(x) = V_0 \exp(-40x^2)$. The final time is $T = 5$ and the time step is $\Delta t = 10^{-2}$, corresponding to $N_T = 500$ time iterations. The space step is set to $\Delta x = 4 \times 10^{-2}$. We report the solution of reference in Ω at final time $T = 5$ for $V_0 = 0$ (free-space FSE), and the solutions in $\Omega_\pm$ after the first Schwarz ($k = 1$) iteration in Fig. 4 (Top-Left) and at convergence ($k = k_\delta$) in Fig. 4 (Top-Right). We also plot in Fig. 4 (Bottom-Left) the error between the mass (resp. total energy) of the reconstructed global solution v (from $u^\pm$) at each Schwarz iteration k and the mass (resp. total energy) of the converged solution $v^{N_T;(k_\infty)}$, i.e.

$$\Delta\mathcal{N}^{(k)} = |\mathcal{N}^{N_T;(k)} - \mathcal{N}^{N_T;(k_\infty)}|\,,$$

and

$$\Delta\mathcal{E}^{N_T;(k)} = |\mathcal{E}^{N_T;(k)} - \mathcal{E}^{N_T;(k_\infty)}|\,,$$

at final time iteration N_T. This shows that the two conservation laws hold at convergence. In Fig. 4 (Bottom-Right), we report the graph of convergence of the SWR method, i.e. the relative ℓ^2-norm error given by (21) as function of k for both the free-space case $V_0 = 0$ and for $V_0 = 100$. The presence of the potential does not really affect the convergence rate. In this first example, we fixed the stopping criterion to an error less than $\delta = 10^{-14}$. From this first example, we can see that the SWR DDM is an efficient convergent algorithm.

We consider the same data as before except that α varies from 0.2 to 1.4, and we fix $V_0 = 0$. We observe on Fig. 5 (Top-Left) that the convergence of the SWR algorithm strongly depends on the value of α : more specifically, the larger α, the slower the convergence. Let us now consider again the same parameters but for the fixed value $\alpha = 0.3$, and we let the time (resp. space) step varies, for $\Delta x = 8/199$ (resp. $\Delta t = 1/40$). We plot in Fig. 5 (Top-Right and Bottom) the convergence rate of the SWR method vs the time and space steps, illustrating that the larger (resp. smaller) the space (resp. time) step, the faster the convergence.

In fact, we can extract some specific information from this test. It is well-known that for classical Schrödinger equations ($\alpha = 2$), the rate of convergence (in the asymptotic regime) of the SWR methods corresponds to the contraction factor K of a fixed point algorithm [4, 5, 6, 8, 17, 30]. We hereafter assume that the contraction factor K for the proposed SWR method is of the form

$$K(\alpha, \Delta t, \Delta x) := \exp\big(-f(\alpha, \Delta t, \Delta x)\big)\,.$$

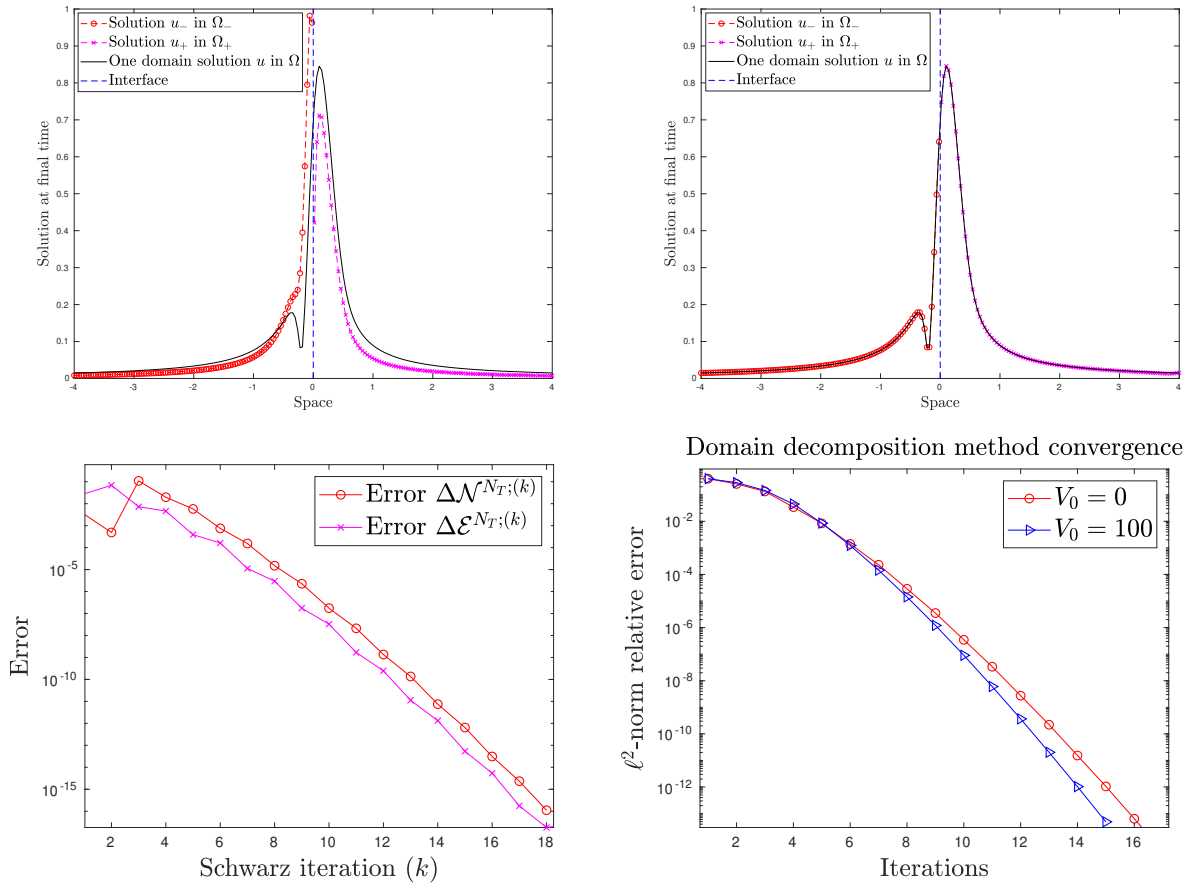

Figure 4: Solutions at final time $T = 5$ (Top-Left) at iteration $k = 1$ and (Top-Right) at convergence $k = k_\delta$. (Bottom-Left) Error on the total mass and total energy at final time, in semi-logscale. (Bottom-Right) Convergence of the SWR method : relative ℓ^2-norm error as a function of Schwarz iterations.

In order to estimate the dependence in Δt and Δx through the function f, at fixed iterations $k = 12, 14, 16$ and Δx, we report in Fig. 6 (Left) the following graph

$$\left\{\Delta t, \log\left|\log\left(K(\alpha, \Delta t, \Delta x)\right)\right|\right\}.$$

We find that this graph is a straight line, with a slope given by ≈ -0.3, that is $-\alpha$. This was numerically confirmed by performing the same test with different values of α. This suggests that the dependence in Δt within the contraction factor is of the form $\propto \exp(-\alpha\Delta t)$. Similarly, in order to estimate the dependence in Δx in K, we report in Fig. 6 (Right) at fixed iterations $k = 11, 12, 13$ and fixed $\Delta t = 1/20$, the following graph

$$\left\{\log(\Delta x), \log\left|\log(K\left(\alpha, \Delta t, \Delta x\right)\right)\right|\right\}.$$

Assuming that the dependence inside the contraction factor is $\propto \Delta x^\beta$, we find a slope ≈ 0.14 which is close to $\beta = \alpha/2$; this allows us to conjecture that the dependence inside the

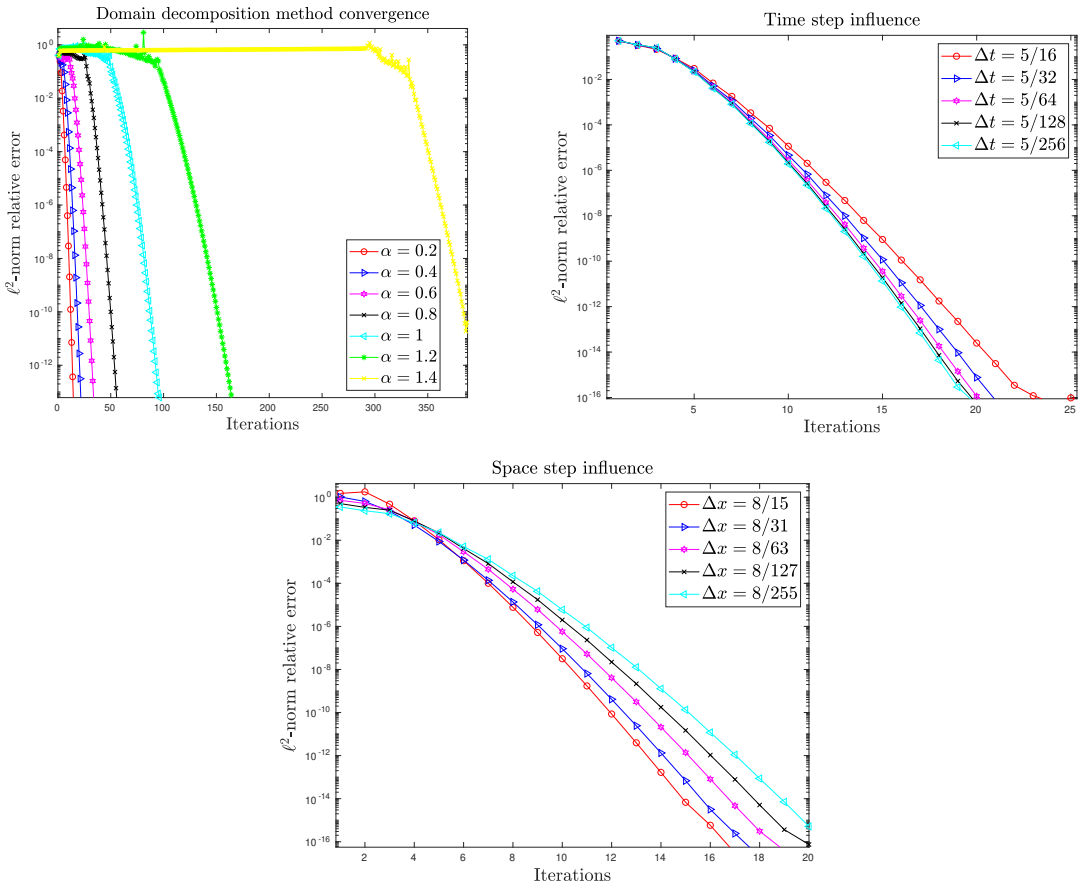

Figure 5: Convergence of the SWR method for different values of α (Top-Left), for different time steps Δt (Top-Right) and for different space discretizations Δx (Bottom).

contraction factor is $\propto \Delta x^{\alpha/2}$, which is actually consistent with the case of the SWR method for the standard Schrödinger equation ($\alpha = 2$) (see e.g. [4, 5, 6, 8, 30]) where is proven the dependence $\propto \Delta x$ inside the function f. This conjecture was yet confirmed through more computations with other values of α. In fine, these experiments, in particular the fact that the convergence rate is a decreasing function of α, lead to the following conjecture.

Conjecture 1. *The convergence rate $K(\alpha, \Delta t, \Delta x)$ of the SWR method* (19) *for the one-dimensional free-space FSE (1) is of the form*

$$K(\alpha, \Delta t, \Delta x) \propto \exp\left(- c(\alpha) e^{-\alpha \Delta t} \Delta x^{\alpha/2} \right),$$

for some positive function c of α.

This conjecture will be mathematically investigated in a future work.

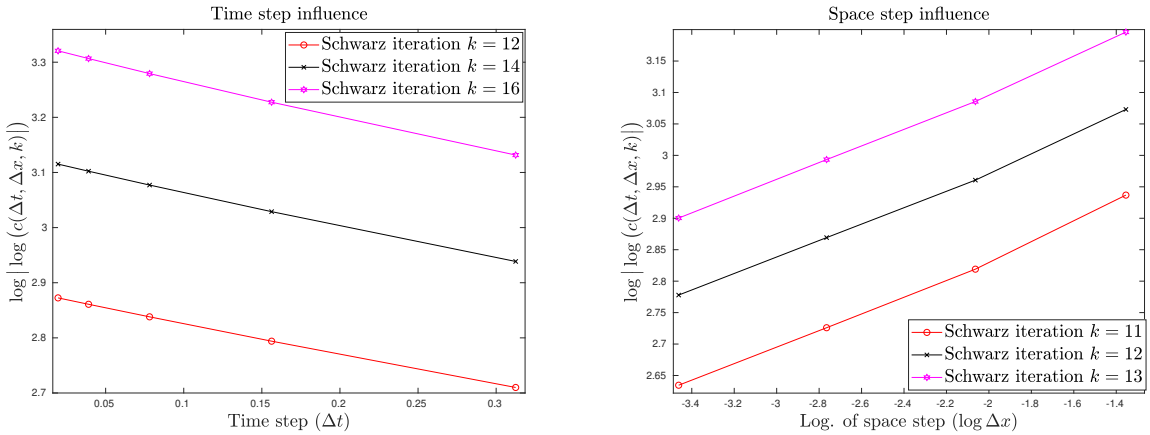

Figure 6: Dependence of the contraction factor K in Δt (Left) and Δx (Right).

4.2. The nonlinear fractional Schrödinger equation

For completeness, we propose an extension of the proposed method to nonlinear fractional Schrödinger equations (NFSE)

$$\mathtt{i}\partial_t u + (-\triangle)^{\alpha/2} u + V(x)u + \mathcal{F}(u)u \;\; = \;\; 0, \;\; u(0,x) = u_0(x), \;\; u(t, \partial\Omega) = 0\,, \qquad (23)$$

where $\mathcal{F}(u)$ is a nonlinear potential. For such an equation, both the mass and the total fractional energy are conserved (see also (27)) when $\Omega := \mathbb{R}^d$.

The extension of the SWR DDM is straightforward, if we use an explicit representation of the nonlinear potential, that is $\mathcal{F}(\boldsymbol{u}_{\pm}^n)$. Denoting by $u_{\pm;i}^{n;(k)}$ the approximate solution at Schwarz iteration k, time t_n and point x_i, the numerical scheme that we propose for the nonlinear case, for $1 \leqslant i \leqslant J/2$, reads in Ω_+

$$\begin{aligned}
&\frac{v_{i;+}^{n+1/2;(k)} + v_{i;+}^{n-1/2;(k)}}{2} = \mathcal{F}(u_{+;i}^{n;(k)}) \\
&\qquad u_{+;i}^{n+1;(k)} = u_{+;i}^{n;(k)} - \frac{\mathtt{i}\Delta t}{2}\Big[\sum_{j\geqslant 1}\big(u_{+;i}^{n;(k)} - u_{+;i+j}^{n;(k)}\big)w_j + \sum_{j\geqslant 1}\big(u_{+;i}^{n+1;(k)} - u_{+;i+j}^{n+1;(k)}\big)w_j \\
&\qquad\qquad \sum_{1\leqslant j\leqslant i-1}\big(u_{+;i}^{n;(k)} - u_{+;i-j}^{n;(k)}\big)w_j + \sum_{j\geqslant i}\big(u_{+;i}^{n;(k)} - u_{-;j}^{n;(k-1)}\big)w_j\Big] \\
&\qquad\qquad\qquad = \frac{\mathtt{i}\Delta t}{2} v_{+;i}^{n+1/2;(k)}(u_{+;i}^{n;(k)} + u_{+;i}^{n+1;(k)}), \qquad (24)
\end{aligned}$$

and as follows in Ω_-

$$\frac{v_{i;-}^{n+1/2;(k)} + v_{i;-}^{n-1/2;(k)}}{2} = \mathcal{F}(u_{+;-}^{n;(k)})$$

$$u_{-;i}^{n+1;(k)} = u_{-;i}^{n;(k)} - \frac{\mathtt{i}\Delta t}{2}\Big[\sum_{j\geqslant 1}\big(u_{-;i}^{n;(k)} - u_{-;i-j}^{n;(k)}\big)w_j + \sum_{j\geqslant 1}\big(u_{-;i}^{n+1;(k)} - u_{-;i-j}^{n+1;(k)}\big)w_j$$
$$+ \sum_{1\leqslant j\leqslant J/2-i}\big(u_{-;i}^{n;(k)} - u_{-;i+j}^{n;(k-1)}\big)w_j + \sum_{j>J/2-i}\big(u_{-;i}^{n;(k)} - u_{+;j}^{n;(k-1)}\big)w_j\Big]$$
$$+ \frac{\mathtt{i}\Delta t}{2}v_{-;i}^{n+1/2;(k)}\big(u_{-;i}^{n;(k)} + u_{-;i}^{n+1;(k)}\big). \quad (25)$$

The discretization of the nonlinearity is based on a relaxation scheme which was developed in [15] for $\alpha = 2$. Here, we fixed the initial values as follows $v_{i;\pm}^{-1/2;(k)} = v_{i;\pm}^{1/2;(k)} = \mathcal{F}(u_{i;\pm}^{0;(k)})$. For the standard integer case, the relaxation scheme scheme allows for a mass and modified total energy conservation for the power-law nonlinearity case $\mathcal{F}(u) = \kappa|u|^{2\sigma}$, where κ is the nonlinearity strength and $\sigma \geqslant 1$ ($\sigma = 1$ corresponds to the cubic case). When discretizing by the relaxation scheme, then the total discrete mass (11) is still conserved as well as the modified discrete fractional total energy defined by

$$\mathcal{E}^n := \frac{1}{2}(\boldsymbol{A}\boldsymbol{u}^n, \boldsymbol{u}^n)_{2,J} + (\boldsymbol{V}\boldsymbol{u}^n, \boldsymbol{u}^n)_{2,J} + \frac{\kappa}{2+2\sigma}(\boldsymbol{v}^{n-1/2}, \boldsymbol{v}^{n+1/2})_{2,J}, \quad (26)$$

where $\boldsymbol{A}$ is the matrix related to the fractional Laplacian and $\boldsymbol{V}$ to the potential. The discretization (26) provides an approximation of the continuous fractional energy given by

$$\mathcal{E}(t) := \frac{1}{2}\int_\Omega \bar{u}(-\triangle)^{\alpha/2}u d\Omega + \int_\Omega V|u|^2 d\Omega + \frac{\kappa}{2+2\sigma}\int_\Omega |u|^{2+2\sigma} d\Omega, \forall t > 0, \quad (27)$$

which is proved to be conserved [11, 12] when $\Omega = \mathbb{R}^d$.

In the following example, we consider the cubic NFSE ($\sigma = 1$) with nonlinearity strength $\kappa = \pm 5, \pm 50$ and fractional exponent $\alpha = 1.9$. The computational domain is $(-5/2, 5/2)$, $\Delta t = 10^{-4}$, $N_T = 5 \times 10^2$, $J = 100$, and the initial data is $\exp(-5x^2 + 10\mathtt{i}x)$. We report the solution for $\kappa = 5$ after the first and last (converged) SWR iterations in Fig. 7, as well as the graph of convergence for the different values of κ. Interestingly, the convergence rate of the SWR method in this case seems independent of the value of κ. This is relatively coherent with the conclusion from the linear case where the potential V does not seem to affect the convergence rate. Here, within the relaxation scheme, the nonlinearity is indeed considered as a potential. The graphs of the relative error for both the discrete mass and modified fractional energy of the converged solution are also represented in Fig. 7 (Bottom-Right) for $\kappa = 5$. This shows that both the mass and modified energy are very well conserved, suggesting that the relaxation scheme [15] is still applicable to the cubic NFSE.

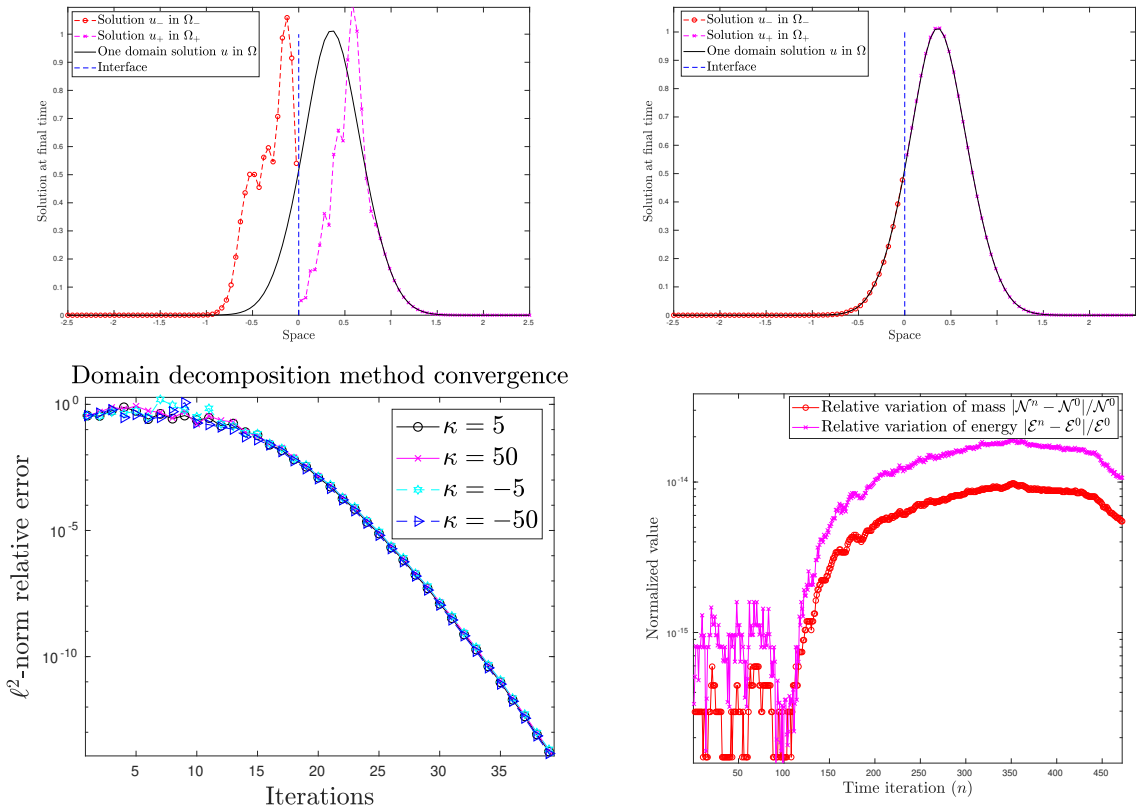

Figure 7: Solutions at final time $T = 0.25$ (Top-Left) at iteration $k = 1$ and (Top-Right) at convergence $k = k_\delta$. (Bottom-Left) Graph of convergence of the SWR method for $\kappa = \pm 5, \pm 50$: relative ℓ^2-norm error as a function of Schwarz iterations k. (Bottom-Right) Mass and energy of the converged solution for $\kappa = 5$.

5. Extension to fractional heat equations

It is worthwhile remarking that the DDM which was proposed in this paper is actually directly applicable to the Fractional Heat Equation (FHE)

$$\partial_t u + (-\triangle)^{\alpha/2} u + V(x)u \;\; = \;\; 0, \;\; u(0,x) = u_0(x), \;\; u(t,\partial\Omega) = 0\,, \tag{28}$$

with $\alpha \in (0,2)$. The FHE has been introduced to model anomalous diffusion [51] when the stochastic process driving the medium is a Lévy α-stable flight. Other applications can also involved nonlinear versions of the FHE as fractional Cahn-Allen [45, 54] and Cahn-Hillard equations [2, 66] where our SWR DDM may apply.

The numerical schemes for solving (28) are trivially adapted from (10) and (15), where now the ℓ^2-norm is naturally not preserved anymore

$$\Big(\boldsymbol{I} + \frac{\Delta t}{2}\boldsymbol{A}_V\Big)\boldsymbol{u}^{n+1} \;\; = \;\; \Big(\boldsymbol{I} - \frac{\Delta t}{2}\boldsymbol{A}_V\Big)\boldsymbol{u}^{n},$$

where $\boldsymbol{A}_V$ is the full real matrix deduced from (7) removing the i-term, and $\|\boldsymbol{u}^{n+1}\|_{2,J} \leqslant \|\boldsymbol{u}^n\|_{2,J}$. It is of course possible to use a standard backward Euler scheme in time following

$$\big(\boldsymbol{I} + \Delta t \boldsymbol{A}_V\big)\boldsymbol{u}^{n+1} \;\; = \;\; \boldsymbol{u}^n \, .$$

The conclusions of Proposition 2.1 remain valid. The SWR DDM derived and analyzed in Section (3) are also still applicable to the fractional heat equation and reads

$$\Big(\boldsymbol{I} + \frac{\Delta t}{2}\boldsymbol{A}_{V,\pm}\Big)\boldsymbol{u}_{\pm}^{n+1;(k)} \;\; = \;\; \Big(\boldsymbol{I} - \frac{\Delta t}{2}\boldsymbol{A}_{V,\mp}^T\Big)\boldsymbol{u}_{\pm}^{n;(k)} + \boldsymbol{F}_{\pm}^{n+1;(k-1)} + \boldsymbol{F}_{\pm}^{n;(k-1)} \, ,$$

where $\boldsymbol{A}_{V,+} = \boldsymbol{A}_{V,-}^T \in \mathbb{R}^{J/2\times J/2}$ and $\boldsymbol{F}_{\pm}^{n;(k-1)} \in \mathbb{C}^{J/2}$ are constructed from (17) and (18) by simply removing the i-term. Alternatively, a backward Euler scheme in time, reads

$$\big(\boldsymbol{I} + \Delta t \boldsymbol{A}_{V,\pm}\big)\boldsymbol{u}_{\pm}^{n+1;(k)} \;\; = \;\; \boldsymbol{u}_{\pm}^{n;(k)} + \boldsymbol{F}_{\pm}^{n+1;(k-1)} \, .$$

As a simple illustration of this DDM over $(-4, 4)$ and $T = 5$, with an initial data given by $u_0(x) = \exp(-20x^2)$, we report in Fig. 9 (Left), the graph of convergence of the DDM method for the heat equation with $\alpha = 0.5$, $V_0 = 0$, $J = 200$ and $\Delta t = 10^{-2}$. In Fig. 9 (Right), the corresponding converged solution is also plotted.

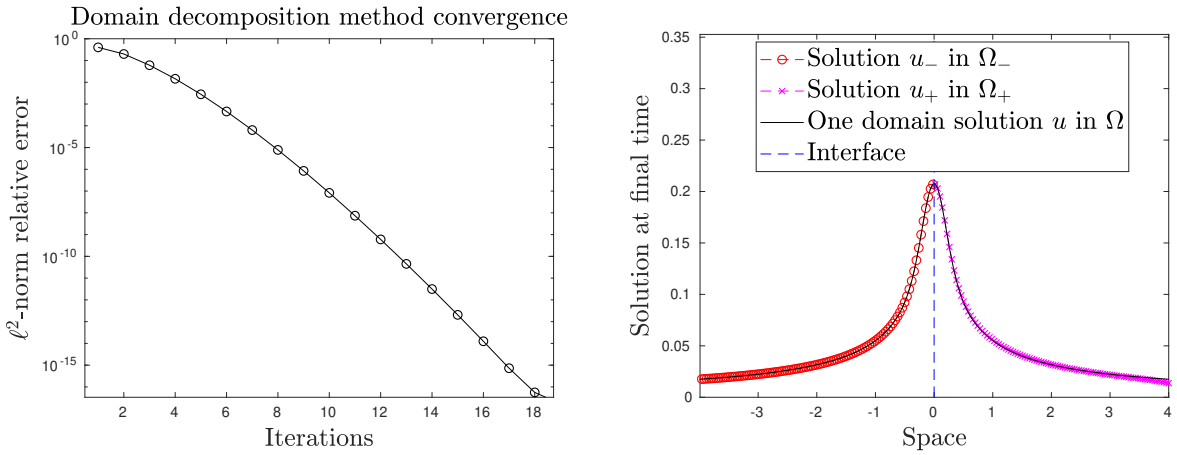

Figure 8: (Left) Convergence of Schwarz waveform relaxation method for the FHE ($\alpha = 0.5$): relative ℓ^2-norm error as a function of the Schwarz iterations k. (Right) Converged solution.

Finally, we compare the rate of convergence of the SWR DDM for the FHE with α close to 2, here $\alpha = 1.99$, and for the standard heat equation (corresponding to $\alpha = 2$) on $(-4, 4)$ with the classical SWR (Dirichlet-based SWR) using a non-overlapping Crank-Nicolson scheme [25]. We take $V(x) = V_0 \exp(-10x^2)$, with $V_0 = 5, 50, 500$, and $J = 200$, $\Delta t = 10^{-3}$, $N_T = 10^2$. Interestingly for large values of V_0, the convergence rate of both SWR methods seems to be comparable. However, the smaller the magnitude of the potential, the slower the convergence rate of the SWR method for the FHE (for $\alpha = 1.99$). Notice that the

SWR method for the FHE can be improved for α close to 2, since in this case the sequence $\{w_j\}$ is rapidly decreasing to 0, suggesting that most of the coefficients could be dropped (corresponding to a localization of the approximate fractional Laplacian) while still keeping a good accuracy.

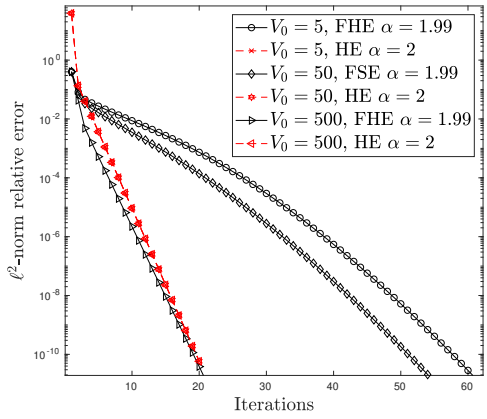

Figure 9: Convergence of Schwarz waveform relaxation method: relative ℓ^2-norm error as a function of Schwarz iterations: comparison between the FHE with $\alpha = 1.99$ and standard heat equation with Crank-Nicolson discretization.

6. Conclusion

In this paper, we have derived, analyzed and implemented a simple DDM for computing in parallel the numerical solution of the one-dimensional linear and nonlinear space fractional Schrödinger equations, as well as fractional heat equation. The convergence of the method was established, as well as its computational complexity. An estimation of its convergence rate was also proposed thanks to numerical experiments and using the standard theory of SWR methods for classical Schrödinger equations. Due to the structure of the fractional Schrödinger operator, the transmission conditions are non-local in space but local in time. In order to improve the efficiency of the method, local-in-space transmission conditions should then be investigated. Regarding the acceleration of the convergence rate, a natural approach would be to develop transparent or absorbing transmission conditions, as commonly done for standard Schrödinger equations, while however keeping locality in time. Future works will also focus on the analysis of the SWR methods for multi-dimensional equations.

References

[1] B. N. Achar, B. T. Yale, and J. W. Hanneken. Time fractional Schrödinger equation revisited. *Adv. Math. Phys.*, 2013:290216, 2013.

[2] M. Ainsworth and Z. Mao. Analysis and approximations of a fractional Cahn-Hilliard equation. *SIAM Journal on Numerical Analysis*, 55:1689–1718, 2017.

[3] M. Al-Khaleel, A.E. Ruehli, and M.J. Gander. Optimized waveform relaxation methods for longitudinal partitioning of transmission lines. *IEEE Transactions on Circuits and Systems*, 56:1732–1743, 2009.

[4] X. Antoine, F. Hou, and E. Lorin. Asymptotic estimates of the convergence of classical Schwarz waveform relaxation domain decomposition methods for two-dimensional stationary quantum waves. *ESAIM Math. Model. Numer. Anal.*, 52(4):1569–1596, 2018.

[5] X. Antoine and E. Lorin. An analysis of Schwarz waveform relaxation domain decomposition methods for the imaginary-time linear Schrödinger and Gross-Pitaevskii equations. *Numer. Math.*, 137(4):923–958, 2017.

[6] X. Antoine and E. Lorin. Multilevel preconditioning technique for Schwarz waveform relaxation domain decomposition method for real- and imaginary-time nonlinear Schrödinger equation. *Appl. Math. Comput.*, 336:403–417, 2018.

[7] X. Antoine and E. Lorin. Asymptotic convergence rates of Schwarz waveform relaxation algorithms for Schrödinger equations with an arbitrary number of subdomains. *Multiscale Science and Engineering*, 1(1):34–46, 2019.

[8] X. Antoine and E. Lorin. On the rate of convergence of Schwarz waveform relaxation methods for the time-dependent Schrödinger equation. *J. Comput. Appl. Math.*, 354:15–30, 2019.

[9] X. Antoine and E. Lorin. ODE-based double-preconditioning for solving linear systems $A^\alpha x = b$ and $f(A)x = b$. *to appear in Numerical Linear Algebra with Applications*, 2021.

[10] X. Antoine, E. Lorin, and Y. Zhang. Derivation and analysis of computational methods for fractional laplacian equations with absorbing layers. *Numerical Algor.*, 2021.

[11] X. Antoine, Q. Tang, and J. Zhang. On the numerical solution and dynamical laws of nonlinear fractional Schrödinger/Gross-Pitaevskii equations. *International Journal of Computer Mathematics*, 95(6-7):1423–1443, 2018.

[12] X. Antoine, Q. Tang, and Y. Zhang. On the ground states and dynamics of space fractional nonlinear Schrödinger/Gross-Pitaevskii equations with rotation term and nonlocal nonlinear interactions. *J. Comput. Phys.*, 325:74–97, 2016.

[13] M. Bologna B. West and P. Grigolini. *Physics of Fractal Operators*. Springer, New York, 2002.

[14] W. Bao and X. Dong. Numerical methods for computing ground state and dynamics of nonlinear relativistic Hartree equation for boson stars. *J. Comput. Phys.*, 230:5449–5469, 2011.

[15] C. Besse. A relaxation scheme for the nonlinear Schrödinger equation. *SIAM J. Numer. Anal.*, 42(3):934–952, 2004.

[16] C. Besse and F. Xing. Domain decomposition algorithms for two-dimensional linear Schrödinger equation. *J. Sci. Comput.*, 72(2):735–760, 2017.

[17] C. Besse and F. Xing. Schwarz waveform relaxation method for one-dimensional Schrödinger equation with general potential. *Numer. Algor.*, 74(2):393–426, 2017.

[18] M. Bhatti. Fractional Schrödinger wave equation and fractional uncertainty principle. *Int. J. Contem. Math. Sci.*, 2:943–950, 2007.

[19] A. H. Bhrawy and M. A. Abdelkawy. A fully spectral collocation approximation for multi-dimensional fractional Schrödinger equations. *J. Comput. Phys.*, 294:462–483, 2015.

[20] I. Carusotto and C. Ciuti. Quantum fluids of light. *Rev. Mod. Phys.*, 85:299–366, 2013.

[21] Y. Cho, H. Hajaiej, G. Hwang, and T. Ozawa. On the Cauchy problem of fractional Schrödinger equation with Hartree type nonlinearity. *Funkcialaj Ekvacioj*, 56(2):193–224, 2013.

[22] J. Dong and M. Xu. Space-time fractional Schrödinger equation with time-independent potentials. *J. Math. Anal. Appl.*, 344(2):1005–1017, 2008.

[23] S. Duo and Y. Zhang. Mass conservative method for solving the fractional nonlinear Schrödinger equation. *Comp. Math. Appl.*, 71:2257–2271, 2016.

[24] A. Elgart and B. Schlein. Mean field dynamics of boson stars. *Commun. Pure Appl. Math.*, 60:500–545, 2007.

[25] M. Gander and L. Halpern. Optimized Schwarz waveform relaxation methods for advection reaction diffusion problems. *SIAM J. Numer. Anal.*, 45(2), 2007.

[26] M.J. Gander. Optimal Schwarz waveform relaxation methods for the one-dimensional wave equation. *SIAM J. Numer. Anal.*, 41:1643–1681, 2003.

[27] M.J. Gander. Optimized Schwarz methods. *SIAM J. Numer. Anal.*, 44:699–731, 2006.

[28] M.J. Gander, L. Halpern, and F. Nataf. Optimal convergence for overlapping and non-overlapping Schwarz waveform relaxation. In *Eleventh International Conference of Domain Decomposition Methods*, pages 27–36, 1999.

[29] B. Guo, Y. Han, and J. Xin. Existence of the global smooth solution to the period boundary value problem of fractional nonlinear Schrödinger equation. *Appl. Math. and Comput.*, 204(1):468–477, 2008.

[30] L. Halpern and J. Szeftel. Optimized and quasi-optimal Schwarz waveform relaxation for the one-dimensional Schrödinger equation. *Math. Models Methods Appl. Sci.*, 20(12):2167–2199, 2010.

[31] X. He and W. Zou. Existence and concentration result for the fractional Schrödinger equations with critical nonlinearities. *Calculus of Variations and Partial Differential Equations*, 55(4), 2016.

[32] B. Hicdurmaz and A. Ashyralyev. A stable numerical method for multidimensional time fractional Schrödinger equation. *Comput. Math. Appl.*, 72:1703–1713, 2016.

[33] L. Hörmander. *Linear Partial Differential Operators*. Springer Verlag, Berlin, 1976.

[34] L. Hörmander. *The Analysis of Linear Partial Differential Operators. III*. Classics in Mathematics. Springer, Berlin, 2007. Pseudo-differential operators.

[35] Y. Huang and A. Oberman. Numerical methods for the fractional Laplacian: a finite difference–quadrature approach. *SIAM J. Numer. Anal.*, 52(6):3056–3084, 2014.

[36] B. L. G. Jonsson J. Fröhlich and E. Lenzmann. Effective dynamics for boson stars. *Nonlinearity*, 20:1031–1075, 2007.

[37] Y. Jiang and X. Xu. Domain decomposition methods for space fractional partial differential equations. *J. Comput. Phys.*, 350:573 – 589, 2017.

[38] A. Q. M. Khaliq, X. Liang, and K. M. Furati. A fourth-order implicit-explicit scheme for the space fractional nonlinear Schrödinger equations. *Numer. Algor.*, 75(1):147–172, 2017.

[39] K. Kirkpatrick and Y. Zhang. Fractional Schrödinger dynamics and decoherence. *Physica D: Nonlinear Phenomena*, 332:41–54, 2016.

[40] D. Kusnezov, A. Bulgac, and G. Dang. Quantum Lévy processes and fractional kinetics. *Phys. Rev. Lett.*, 82:1136–1129, 1999.

[41] M. Kwásnicki. Ten equivalent definitions of the fractional laplace operator. *Fractional Calculus and Applied Analysis*, 20(1):7–51, 2017.

[42] N. Laskin. Fractals and quantum mechanics. *Chaos*, 10:780–790, 2000.

[43] N. Laskin. Fractional quantum mechanics. *Phys. Rev. E*, 62:3135–3145, 2000.

[44] N. Laskin. Fractional quantum mechanics and Lévy path integrals. *Phys. Lett. A*, 268:298–304, 2000.

[45] S. Lee and D. Lee. The fractional Allen-Cahn equation with the sextic Ginzburg-Landau potential. *Appl. Math. Comput.*, 351:176–192, 2019.

[46] X. Liang, A.Q.M. Khaliq, H. Bhatt, and K.M. Furati. The locally extrapolated exponential splitting scheme for multi-dimensional nonlinear space-fractional Schrödinger equations. *Numer. Algor.*, 74(4):1–20, 2017.

[47] A. Lischke, G. Pang, M. Gulian, F. Song, C. Glusa, X. Zheng, Z. Mao, W. Cai, M.M. Meerschaert, M. Ainsworth, and G. E. Karniadakis. What is the fractional Laplacian? A comparative review with new results. *J. Comput. Phys.*, 404, 2020.

[48] A. Lomin. Fractional-time quantum dynamics. *Phys. Rev. E*, 62:3135–3145, 2000.

[49] E. Lorin and S. Tian. A numerical study of fractional linear algebraic systems. *Math. Comput. Simul.*, 182:495–513, 2021.

[50] B. C. Mandal. A time-dependent Dirichlet-Neumann method for the heat equation. In *Domain Decomposition Methods in Science and Engineering XXI*, pages 467–475. Springer International Publishing, 2014.

[51] R. Metzler and J. Klafter. The random walk's guide to anomalous diffusion: a fractional dynamics approach. *Physics Reports*, 339:1–77, 2000.

[52] A. Mohebbi, M. Abbaszadeh, and M. Dehghan. The use of a meshless technique based on collocation and radial basis functions for solving the time fractional nonlinear Schrödinger equation arising in quantum mechanics. *Eng. Anal. Bound. Elem.*, 37:475–485, 2013.

[53] M. Naber. Time fractional Schrödinger equation. *J. Math. Phys.*, 45:3339–3352, 2004.

[54] Y. Nec, A. A. Nepomnyashchy, and A. A. Golovin. Front-type solutions of fractional Allen-Cahn equation. *Physica D: Nonlinear Phenomena*, 237(24):3237–3251, 2008.

[55] E. Di Nezza, G. Palatucci, and E. Valdinoci. Hitchhiker's guide to the fractional Sobolev spaces. *Bulletin des Sciences Mathématiques*, 136(5):521–573, 2012.

[56] L. Nirenberg. *Lectures on Linear Partial Differential Equations.* American Mathematical Society, Providence, R.I., 1973.

[57] F. Pinsker, W. Bao, Y. Zhang, H. Ohadi, A. Dreismann, and J. J. Baumberg. Fractional quantum mechanics in polariton condensates with velocity-dependent mass. *Phys. Rev. B*, 92:195310, 2015.

[58] I. Moret R. Garrappa and M. Popolizio. Solving the time-fractional Schrödinger equation by Krylov projection methods. *J. Comput. Phys.*, 293:115–134, 2015.

[59] M. Ran and C. Zhang. A conservative difference scheme for solving the strongly coupled nonlinear fractional Schrödinger equations. *Commun. Nonlin. Sci. Numer. Simul.*, 41:64–83, 2016.

[60] X. Shang, J. Zhang, and Y. Yang. On fractional Schrödinger equation in $\mathbf{R}^n$ with critical growth. *J. Math. Phys.*, 54(12), 2013.

[61] V. Tarasov. Fractional Heisenberg equation. *Phys. Lett. A*, 372:2984–2988, 2006.

[62] K. Teng. Multiple solutions for a class of fractional Schrödinger equations in $\mathbf{R}^n$. *Nonlinear Anal. Real World Appl.*, 21(1):76–86, 2015.

[63] D. Wang, A. Xiao, and W. Yang. Crank-Nicolson difference scheme for the coupled nonlinear Schrödinger equations with the Riesz space fractional derivative. *J. Comput. Phys.*, 242:670 – 681, 2013.

[64] D. Wang, A. Xiao, and W. Yang. Maximum-norm error analysis of a difference scheme for the space fractional CNLS. *Appl. Math. Comput.*, 257:241 – 251, 2015. Recent Advances in Fractional Differential Equations.

[65] S. Wang and M. Xu. Generalized fractional Schrödinger equation with space-time fractional derivatives. *J. Math. Phys.*, 48(4):043502, 2007.

[66] Z.F. Weng, S.Y. Zhai, and X.L. Feng. A Fourier spectral method for fractional-in-space Cahn-Hilliard equation. *Applied Mathematical Modelling*, 42:462–477, 2017.

[67] B. West. Quantum Lévy propagators. *J. Phys. Chem. B*, 104:3830–3832, 2000.

[68] L. Zhang, C. Li, H. Zhong, C. Xu, D. Lei, Y. Li, and D. Fan. Propagation dynamics of super-Gaussian beams in fractional Schrödinger equation: from linear to nonlinear regimes. *Opt. Express*, 24(13):14406–14418, 2016.

[69] Y. Zhang, H. Zhong, M.R. Belić, N. Ahmed, Y. Zhang, and M. Xiao. Diffraction-free beams in fractional Schrödinger equation. *Sci. Rep.*, 6:23645, 2016.